

Article

Methodology for the Automatic Inventory of Olive Groves at the Plot and Polygon Level

Cristina Martínez-Ruedas ^{1,*}, José Emilio Guerrero-Ginel ²  and Elvira Fernández-Ahumada ³ 

¹ Department of Electronic and Computer Engineering, University of Cordoba, 14014 Cordoba, Spain

² Department of Animal Production, University of Cordoba, 14014 Cordoba, Spain; pa1gugij@uco.es

³ Department of Mathematics, University of Cordoba, 14014 Cordoba, Spain; g82feah@uco.es

* Correspondence: z42maruc@uco.es; Tel.: +34-670514255

Abstract: The aim of this study was to develop and validate a methodology to carry out olive grove inventories based on open data sources and automatic photogrammetric and satellite image analysis techniques. To do so, tools and protocols have been developed that have made it possible to automate the capture of images of different characteristics and origins, enable the use of open data sources, as well as integrating and metadating them. They can then be used for the development and validation of algorithms that allow for improving the characterization of olive grove surfaces at the plot and cadastral polygon scales. With the proposed system, an inventory of the Andalusian olive grove has been automatically carried out at the level of cadastral polygons and provinces, which has accounted for a total of 1,519,438 hectares and 171,980,593 olive trees. These data have been contrasted with various official statistical sources, thus ensuring their reliability and even identifying some inconsistencies or errors of some sources. Likewise, the capacity of the Sentinel 2 satellite images to estimate the FCC at the cadastral polygon, parcel and 10×10 m pixel level has been demonstrated and quantified, as well as the opportunity to carry out inventories with temporal resolutions of approximately up to 5 days.

Keywords: automatic olive inventories; visual recognition; open data; Sentinel; photogrammetric



Citation: Martínez-Ruedas, C.; Guerrero-Ginel, J.E.; Fernández-Ahumada, E. Methodology for the Automatic Inventory of Olive Groves at the Plot and Polygon Level. *Agronomy* **2022**, *12*, 1735. <https://doi.org/10.3390/agronomy12081735>

Academic Editor: Baohua Zhang

Received: 17 June 2022

Accepted: 20 July 2022

Published: 22 July 2022

Publisher's Note: MDPI stays neutral with regard to jurisdictional claims in published maps and institutional affiliations.



Copyright: © 2022 by the authors. Licensee MDPI, Basel, Switzerland. This article is an open access article distributed under the terms and conditions of the Creative Commons Attribution (CC BY) license (<https://creativecommons.org/licenses/by/4.0/>).

1. Introduction

The olive tree is one of the most representative crops in the Mediterranean basin closely linked to the economy and culture of the region. Worldwide, the Mediterranean basin is the producer of 99% of olive oil and the consumer of 87% [1].

Traditional olive groves have been and still are a very important component of the Mediterranean landscape. To a considerable extent we could classify them as forests that produce an important range of ecosystem services: healthy food, biodiversity, living soils, carbon sequestration, culture, employment, life in villages, etc. Particularly with regard to olive grove landscapes, the EU has shown great interest in their conservation through strategies such as the European Landscape Convention [2], developing a specific tool for the protection and management of olive groves.

The lack of economic sustainability is causing traditional olive groves to be at serious risk of survival, disappearing on many occasions. More recently, this crop has been changing from traditional rainfed olive groves with a low density of trees (less than 100 trees per hectare) to olive groves of medium and high density, mostly associated with the introduction of irrigation, which is also promoting the substitution of various crops (wheat, barley, sunflower, cotton) by high-density olive groves [3,4]. All this is causing major changes in the management of the olive groves, especially in their intensification, as well as in the economic, social and environmental impacts.

These changes have been strongly noted in one of the main olive-growing regions in the world, Andalusia. Figure 1 and Table 1 show the difference in olive grove areas

between 2015 and 2018. In general, there has been an increase in high-density plantations to the detriment of low ones [5].

Table 1. Olive grove area (ha) per year and plantation density (trees/ha). Source: Analysis of the density in olive plantations in Andalusia. Regional Ministry of Agriculture, Livestock and Fisheries.

Year	<80	80–139	140–399	400–799	800–1000	>1000	Unspecified
2015	111,191	687,220	659,600	35,860	1925	16,355	11,953
2016	108,921	688,689	674,750	38,484	2417	17,930	4659
2017	105,560	682,551	690,029	39,148	2284	23,788	8065
2018	103,257	675,352	711,594	39,889	2564	35,268	10,206

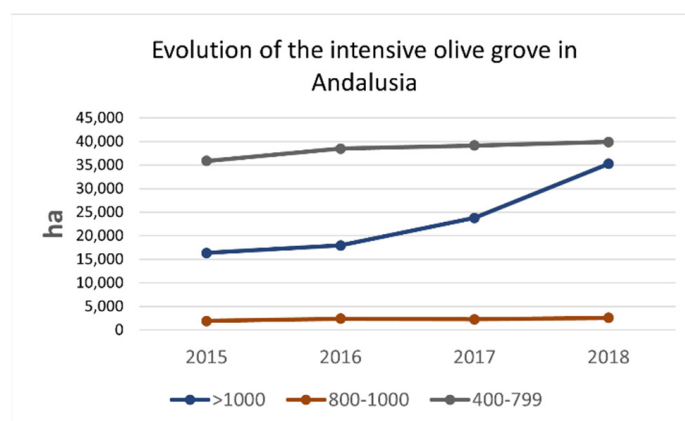


Figure 1. Evolution of the intensive olive grove in Andalusia. Source: Analysis of density in olive plantations in Andalusia. Regional Ministry of Agriculture, Livestock and Fisheries.

Studies such as [3] indicate that this is causing a high environmental impact, among which the problems derived from water needs stand out. However, there is also evidence that the intensification of deficit irrigation has improved carbon sequestration, as investigated by [6], through the modeling of the implications of climate variability and agricultural management on the productivity and environmental performance of olive crops in the Mediterranean. In addition, an increase in such intensification would increase irrigation needs. For this reason, it is becoming more and more necessary to be able to systematize the monitoring of olive tree density with detailed and permanently updated information in large areas. Studies such as [7,8] show the need to provide more detailed information on olive farming practices and to make and quantify proposals to increase specific sustainable practices at the farm level [9].

In this regard, there are numerous publications related to data-capture mechanisms in the field and the use of platforms for their management and visualization [10–15]. In a complementary way, important efforts are being made to create common data spaces in the agricultural field [16–22], which try to overcome the existing barriers regarding the global management of data. The main obstacles found are the following: the complexity of data management [23], the lack of interoperability [16,17,22], the insufficiency of storage units and processing platforms [24,25], as well as the scarcity of reference architectures [23,26–30]. Overcoming these limitations would make it possible to take full advantage of the potential of data analysis and management, strengthening the capabilities of decision-making support systems.

Further, the characterization and monitoring of large areas of crops is becoming a key factor to improving and supporting decision-making. The combination of remote data with ground measurements, obtained from interpretations of high spatial resolution aerial photogrammetry through image analysis, significantly improves the ability to study land processes. In this line, different studies are being promoted, as is the case of [31]

where a methodology for landscape sampling, mapping and characterization of a complex agroforestry system in sub-Saharan Africa is provided.

Therefore, the use of remote sensing has an increasingly important role in the continuous, effective, precise and complete monitoring of large areas, being key in the decision-making processes of agroforestry management [32,33]. It allows crop mapping to be carried out at a low cost and with high frequency, which makes it possible to extend these studies [6–8] to large areas.

For this reason, an aspect of great importance is the possibility of using the synergies between automated procedures to identify and characterize the different ecological units in olive groves from very high resolution images, such as orthophotos with a spatial resolution of 0.5 m or superior. The analyses carried out with satellite images of lower spatial resolution could substantially improve their usefulness and accuracy if models based on spectral mixtures were developed using previous segmentations carried out with image analysis techniques. These studies would make it possible to complement the temporal resolutions of the systems for obtaining digital aerial orthophotography, such as the National Plan for Aerial Orthography (PNOA) [34], whose update period is every three years, which makes it impossible to update inventories periodically.

Regarding the treatment and processing of satellite images, there are platforms such as Google Earth Engine (GEE), which provide easy access to a wide catalogue of images, including those captured by the Sentinel 2-MSI (MultiSpectral Instrument) satellites, and allow for the extraction of relevant vegetation indices in a simple way [35]. Vegetation indices are capable of monitoring crop growth with high-resolution satellite images [36]. Among these indices, the NDVI (Normalized Difference Vegetation Index) has been defined as a good tool to indicate significant changes in land use and cover [37,38]. NDVI shows better results than other indices such as the adjusted vegetation index to the ground (SAVI) [38] and is one of the most widespread, due to its simplicity and availability [39,40]. In addition, according to [41], the analysis of the NDVI for the estimation of the surface of the crops and the qualitative evaluation of these with hydric stress, can lead to an optimization in irrigation management systems.

Thus, it is very important to be able to automate the inclusion of new data, coming from: (i) high-resolution aerial photogrammetry image analysis, such as the crown area, Fraction Canopy Cover (FCC), tree density or the identification of different typologies; (ii) analysis of the NDVI at the pixel and sub-pixel level; (iii) existing open data sources such as the Geographic Information System of Agricultural Parcels SIGPAC [42], the Andalusian Phytosanitary Information and Alert Network RAIF [43] and the Integrated Treatments in Andalusia in Agriculture TRIANA [44]. Furthermore, it is necessary to enable the creation of common data spaces that make it possible to value the tools for the conservation of the olive grove and the detection of changes in its management.

In addition, the processing of measurements from high-resolution aerial frames is very useful for improving the interpretation of satellite images; they provide field data from which it is possible to calibrate the models. Recent studies have focused on the development of tools to generate automated agroforestry inventories for the analysis of large areas [31]. These allow us to calibrate and optimize the analyses carried out with lower resolution satellite images, which are needed in order to complement the studies with spectral mixture analysis techniques of automatic pixel analysis, to improve feature extraction at the olive tree level. Nevertheless, further work is still necessary to delve further into in order to optimize results. In this study, the FCC-NDVI relationship has been evaluated.

We can summarize that it is necessary to obtain detailed information on large olive grove areas, having the plot as the sampling unit and, where appropriate, scaling it to larger territories, which will make it possible to carry out studies at the farm level and characterize the ecosystem services of the olive grove crop providing tools to help decision making.

In this regard, the general objective of the work was to develop and validate a methodology to carry out olive grove inventories based on automatic analysis techniques of

photogrammetric images of PNOA, satellite images of the Sentinel constellation and open data sources.

2. Materials and Methods

2.1. Study Area

The study has been carried out in 11,488 olive grove polygons, which occupy a total of 1,519,438 ha (shown in red in Figure 2), which represents 92% of the total olive grove cultivation in Andalusia. The area was divided into eight zones that correspond to the 8 provinces of Andalusia, thus covering the most widespread varieties such as Picual, Hojiblanca, Manzanilla Verdial, Lechín, Empeltre, Blanqueta, Farga and Arbequina, as well as different plantation frameworks.

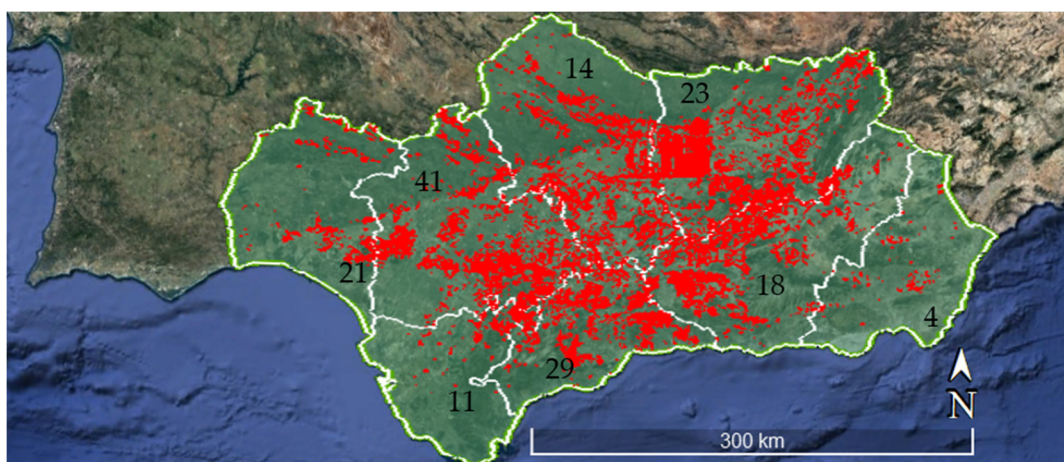


Figure 2. Distribution of hectares where the characterization of olive groves has been carried out. Source: SIGPAC Regional Ministry of Agriculture, Livestock and Fisheries.

2.2. Data Set

The set of high-resolution images used to characterize the olive grove comes from aerial orthophotographs of the PNOA [34] obtained by photogrammetric flights with a high-resolution digital camera. This image dataset has a spectral resolution of 3 bands (blue, green, and red), a radiometric resolution of 12 bits per band, and a spatial resolution of 50 cm.

To obtain the NDVI, images from Sentinel 2 [45] have been used, which provide multispectral data with 13 bands in the visible, near-infrared and short-wave infrared part of the spectrum. They have a spatial resolution of 10 m and a temporal resolution of approximately 5 days.

The contrast and validation of the data was carried out through manual counts and information from the RAIF of olive grove plots [43].

Geospatial and crop data were obtained from SIGPAC [42] and varietal data from TRIANA [43].

The different data were taken for the time interval between 1 January 2019 and 31 December 2019. This interval was selected based on the dates of the most recent PNOA photos at the time of the study, which dated from 2019.

2.3. Programming Languages

The programming languages and the specific processes for which they have been used are as follows:

- MATLAB 2021a (9.10) with two libraries, the Image Analysis Processing toolbox [46] and openearthtools [47], was used for:
 - i. High resolution digital image processing.
- Python 3.6.13 was used for:

- i. Obtaining NDVI data through the Google Earth Engine platform [35]
- ii. The creation of linear regression models.
- iii. The calibration of the results.
- Python 3.8.5 was used for:
 - i. Automatic acquisition of PNOA images.
 - ii. The identification of the area of interest through shapefile files of the geographic information system of agricultural parcels (SIGPAC).
 - iii. Development of APIs for the integration of different open data sources (SIGPAC, RAIF, TRIANA)
 - iv. Data cleaning and preprocessing.

2.4. Procedure

The first step was to adapt and validate the tool developed in the study [48] for the case of olive groves. Subsequently, the olive grove inventory was created from the data obtained in the image processing with the validated tool. Then, the integration of metadata from different open data sources such as SIGPAC, RAIF and TRAINA was carried out. Finally, with the information generated in the inventory, the FCC-NDVI relationship was evaluated at the polygon, plot, and pixel levels.

2.4.1. Validation of the Tool for Olive Groves

In order to validate the tool, the following steps were carried out: (i) manual counts of 33 olive grove plots chosen at random from the set of olive groves in Andalusia (Figure 3); (ii) checks by an observer on the FCC mask obtained by the tool to validate the FCC (Figure 4).

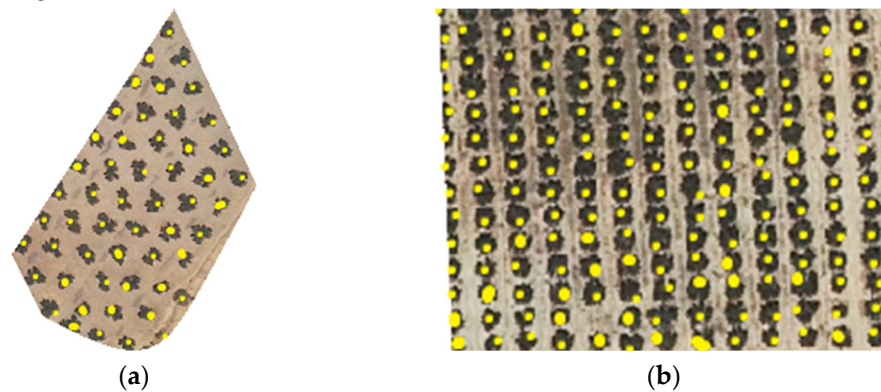


Figure 3. Example of the manual counting of olive grove plots with different plantation frameworks: (a) traditional olive groves; (b) intensive olive groves.

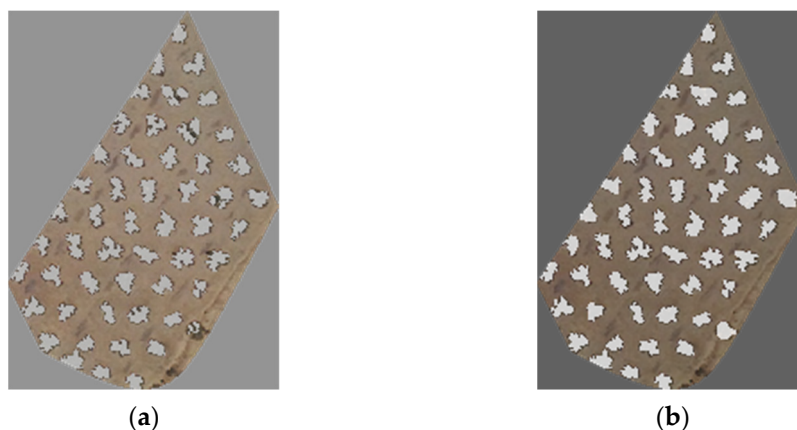


Figure 4. Example of observer correction in photo: (a) FCC calculated by the tool; (b) FCC corrected by the observer.

2.4.2. Creation of an Inventory of Olive Groves

Figure 5 shows a summary of the methodology followed to prepare the inventory. Each of the modules is detailed below.

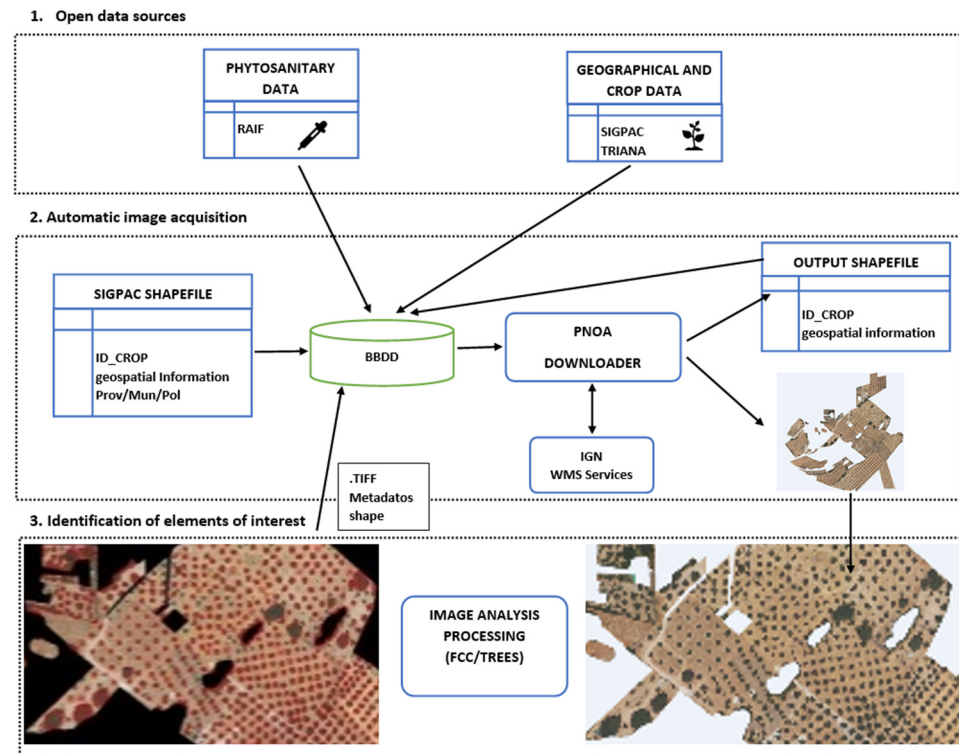


Figure 5. Characterization of the olive grove through PNOA orthophotos of 0.5×0.5 m resolution.

1. Open data sources

The data sources consulted to extract olive grove information were: the Andalusian Phytosanitary Alert Network (RAIF) [43] for phytosanitary information and the Geographic Information System for Agricultural Parcels (SIGPAC) [42,49] and the TRIANA program [44] for geographic and crop information.

RAIF is a set of open data obtained from the monitoring of pests and diseases in the biological control stations, in addition to generic crop information. The data are displayed in Excel files by crop type from 2006 to 2021. The information is updated every week. The main parameters selected for this study were crop type, cultivated area, tree density and crown diameter. These parameters have been used for the automatic validation of the methodology.

TRIANA is a computer program for crop management, in addition to phytosanitary information it provides crop information. The information provided by this data source is the following: crop type, cultivated area, irrigation, nearest climatic season, planting frame, main variety, planting date, secondary variety and planting date. This information has been contrasted and included in the inventory.

The SIGPAC allows the geographic identification of parcels declared by farmers and ranchers. It is accessible through WMS services [49]. The land is sectorized, the smallest unit to be treated in this study is the plot (PROV;NUM;POL;PLOT). By selecting such a sector, the relevant information of the sector is obtained, such as geospatial information, land use, cultivated area, irrigated area and soil slope. The geospatial information provided has been used to automate the download of high resolution images, and land use to identify the area of interest (AOI).

From the different data sources, aspects such as complexity, access limitations, automation capacity, temporal and spatial frequencies, as well as the available time range

were analyzed. After that, data acquisition was automated, carrying out temporally and geographically limited tests with the aim of evaluating the availability and access to the data. Finally, different analysis, preprocessing and cleaning techniques were used, erroneous data were eliminated through Random Forest techniques [50] and missing values were imputed through the `imputeTS` and `missForest` libraries [51]. Lastly, to check the consistency of the data, the data from the different sources were compared, eliminating non-coherent data, thus generating a unified access point for reliable and contrasted agronomic data.

2. Automatic image acquisition

This module automates the downloading, identification and delimitation of study areas from PNOA images for different ecosystems or crops and zones, obtaining a high-resolution image of each polygon/plot and a shapefile with geographic and crop information.

The image download procedure was as follows:

- i. Geospatial and crop information of the area of interest was obtained from the SIGPAC shapefiles.
- ii. The database stores geospatial and crop information at the polygon and/or plot level.
- iii. The PNOA Downloader script takes the geospatial information from the DB and will call the IGN WMS services to download the orthophotography.
- iv. The PNOA Downloader script will generate two outputs: the orthophoto of the polygon/plot with the AOI of the selected crop (olive grove for this particular study) and a shapefile with metadata.
- v. This processed information will be saved in the olive grove data inventory for later interpretation by the tool for precise olive grove characterization.

3. Identification of elements of interest

Image analysis techniques were used for preprocessing [52,53], segmentation [54,55] and classification [56]. In addition, specific developments carried out in previous studies [48] were used to identify the elements of interest in the high-resolution images obtained in point 2. Based on the regularity present in the olive grove, false positives were considered to be those elements whose area or eccentricity were much higher than the average of the detected objects, which allowed for the elimination of elements of other species. As a result, a .TIFF image was obtained with the identified elements and a shapefile with metadata per polygon, thus obtaining automated information on the number of trees, FCC, tree density and tree canopy area. These data obtained from the interpretation of the images were stored in the database to form part of the olive grove data inventory.

2.4.3. FCC-NDVI Evaluation

The evaluation of the FCC-NDVI relationship was carried out considering the polygon and geographical area of the whole Andalusia as the sampling unit and also another approximation with the pixel sampling unit and the geographical area as a plot.

The steps followed are detailed below:

- i. Polygon-level study. The polygon was taken as the sampling unit and the different months of the year 2019 and provinces were evaluated. For this calculation, the mean values of the NDVI of the polygons were taken for each month and the FCC obtained in the characterization of olive groves through orthophotos of the PNOA of 2019. A total of 10,031 polygons were used.
- ii. Plot-level study. The plot was taken as the sampling unit. The evaluation was carried out with a subset of plots from one of the provinces. In the same way as for the polygon, the mean values of the NDVI of the plots for the summer months and the FCC obtained in the characterization of the olive grove through orthophotos of the PNOA of 2019 were taken. A total of 287 plots were used.
- iii. Pixel-level study. Finally, a pixel-level study was carried out, selecting a plot (PROV_14, NUM_900,POL_18,PLOT_14) with diversity in terms of plantation frames and a Sentinel image corresponding to the month of August 2019. This evaluation was

carried out by comparing the mean NDVI of each pixel of the Sentinel image, with the pixels of a 10×10 m resolution image generated from the FCC obtained in the characterization of olive groves. An image with a size of 95×57 pixels was used (see Figure 6).

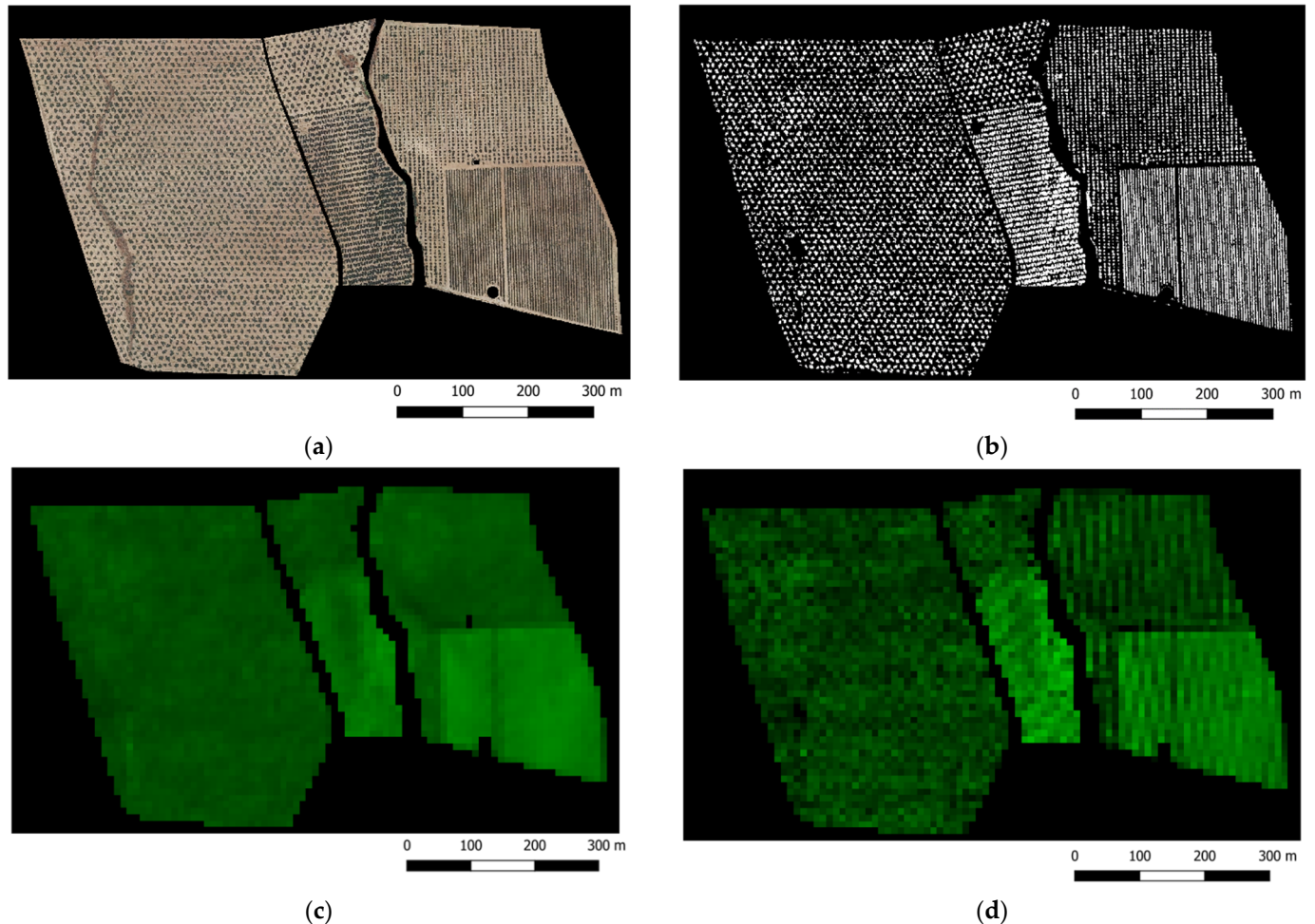


Figure 6. Plot used for the evaluation of the FCC-NDVI at the pixel level. (a) Input image with the olive grove AOI; (b) Image with the FCC calculated by the olive grove tool; (c) Sentinel NDVI image for the date 2 August 2019; (d) Generated NDVI image from image (b).

In all the procedures, it has been considered that the FCC does not present significant variability in one year.

Figure 7 shows the methodology followed to develop the FCC estimation model from the NVDI.

1. Olive grove data extraction

From the olive grove data inventory, the shapefile (shp) files were obtained with the necessary geographic information to obtain the NDVI by remote sensing and the FCC of the polygons and plots for the validation data.

2. Remote sensing data

A Python script was developed that obtained the $NDVI_{mean}$ time series for each plot and polygon from the ShapeFile obtained in the characterization of the olive grove, as well as the images necessary for the evaluation at the pixel level.

3. Validation data

The data considered as real for the calibration and validation of the model were extracted from the FCC obtained in the olive grove characterization.

4. Data analysis

The data collected were grouped by province and month and two simple linear regression models were evaluated to model the relationship between FCC and NDVI: scikit-learn and statsmodels approach (Equation (1))

$$FCC = \beta_1 \cdot NDVI_{mean} + \beta_0 \quad (1)$$

To evaluate the model, the data were divided into two groups: a training group for calibration, in which 80% of the data were used, and a test group, with the remaining data, to evaluate the capacity of the model prediction. The goodness of fit of the model was evaluated using the coefficient of determination (R-squared), the *p*-value statistics were determined (using the F-Test), and the performance of the model was evaluated using the mean squared error (rmse). After generating the model, the confidence interval was used to measure the uncertainty associated with the prediction.

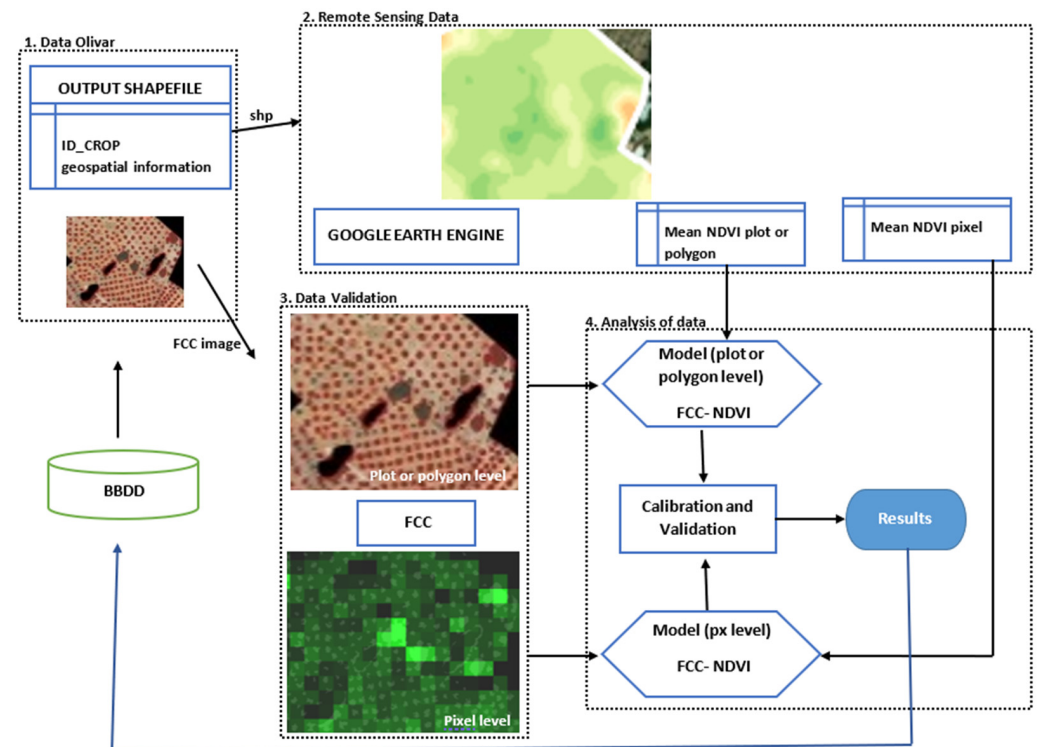


Figure 7. General methodology for estimating FCC in olive groves.

3. Results

3.1. Validation of the Tool for Olive Groves

Table 2 shows the results of the estimation and real value of the number of trees and FCC, as well as the relative error of the 33 plots where the manual counts were made.

As an example, Figure 8 shows the results of four plots (PROV-14, MUN-900, POL-40, PLOT-60; PROV-23, MUN-60, POL-3, PLOT-88; PROV-14, MUN-57, POL-1, PARC-58; PROV-14, MUN-57, POL-2, PARC-49), where the ability of the tool to measure olive groves with different plantation frameworks as well as treeless areas is appreciated.

Table 2. Results of the validation of the tool for olive groves in 33 plots.

PROV	MUN	POL	PLOT	No. of Estimated Trees	No. of Real Trees	Relative Error	FCC Estimated	FCC Real	Relative Error
Córdoba	900	32	43	576	581	0.009	2315.00	2545.75	9.064
Córdoba	900	40	45	759	783	0.030	6795.00	6377.50	6.546
Córdoba	900	40	59	485	480	0.011	1908.25	1959.25	2.603
Córdoba	19	12	77	3207	3173	0.011	56,190.25	57,106.75	1.605
Córdoba	55	9	79	53	53	0.000	1021.25	1105.75	7.642
Córdoba	56	30	84	418	475	0.121	7844.75	7840.00	0.061
Córdoba	57	1	20	391	384	0.018	5837.50	6143.25	4.977
Córdoba	57	1	24	447	442	0.012	7237.50	7439.25	2.712
Córdoba	57	1	58	495	526	0.059	10,169.75	10,360.25	1.839
Córdoba	57	2	50	279	280	0.002	5731.00	5752.50	0.374
Jaén	1	10	365	519	536	0.032	15,946.75	15,953.50	0.042
Jaén	2	4	30	458	454	0.010	6539.00	6539.00	0.000
Jaén	2	10	245	258	235	0.097	3181.75	3108.25	2.365
Jaén	2	11	256	266	262	0.014	3529.50	3610.25	2.237
Jaén	2	17	274	341	368	0.072	10,360.25	10,383.75	0.226
Jaén	2	21	236	199	197	0.011	3053.00	3123.50	2.257
Jaén	2	23	86	342	310	0.102	6587.75	6790.75	2.989
Jaén	2	29	30	390	394	0.010	5100.00	5115.75	0.308
Jaén	2	31	202	272	248	0.097	4580.00	4631.75	1.117
Jaén	2	32	137	290	281	0.033	6149.25	6152.75	0.057
Jaén	2	52	176	413	405	0.019	11,923.75	11,923.75	0.000
Jaén	2	56	29	468	450	0.041	9426.50	9465.75	0.415
Jaén	2	64	20	1902	1886	0.008	34,505.00	34,571.25	0.192
Jaén	2	66	76	1339	1303	0.028	14,844.50	14,392.75	3.139
Jaén	2	71	148	696	681	0.023	17,895.25	17,728.75	0.939
Jaén	2	83	15	2212	2105	0.051	57,297.75	57,328.25	0.053
Jaén	15	6	443	167	158	0.054	3849.75	3860.00	0.266
Jaén	17	23	4	788	766	0.029	25,289.25	25,089.75	0.795
Jaén	26	15	115	1776	1733	0.025	37,741.25	37,676.25	0.173
Jaén	38	5	279	658	666	0.012	13,617.25	13,495.50	0.902
Jaén	53	5	52	317	320	0.010	34,764.50	34,477.50	0.832
Jaén	53	12	3	908	835	0.088	11,470.75	11,916.00	3.737
Jaén	53	43	8	691	542	0.274	10,750.25	11,021.50	2.461

3.2. Creation of Inventories of Olive Groves

After the validation of the developed automatic analysis tool, the olive grove area of Andalusia as a whole was characterized. Table 3 collects the detail of the entire surface characterized by the olive grove tool. The columns Processed Surface, FCC and number of trees, are the data calculated by the automatic analysis tool. The Total Surface column corresponds to the total hectares of olive groves by province, with data collection from the olive grove production capacity carried out by the Andalusian Government for the 2021–2022 campaign.

Table 3. Summary of the characterized olive grove area.

Province_ID	Polygons	Processed Surface (ha)	FCC (ha)	No. of Trees	Total Surface, (ha)
4_Almería	1549	18,892	6045.44	2,542,010	22,092
11_Cádiz	542	29,088	7272.00	2851,288	30,220
14_Córdoba	1767	350,086	73,518.06	39,785,516	370,124
18_Granada	1820	182,918	45,250.26	21,474,448	205,683
21_Huelva	926	33,299	9656.71	3,707,114	35,710
23_Jaén	1375	532,741	111,875.61	57,981,776	587,932
29_Málaga	1653	136,501	34,125.25	14,663,327	140,864
41_Sevilla	1856	235,913	44,202.54	28,975,114	251,340
TOTAL	11,488	1,519,438	331,945.87	171,980,593	1643,965

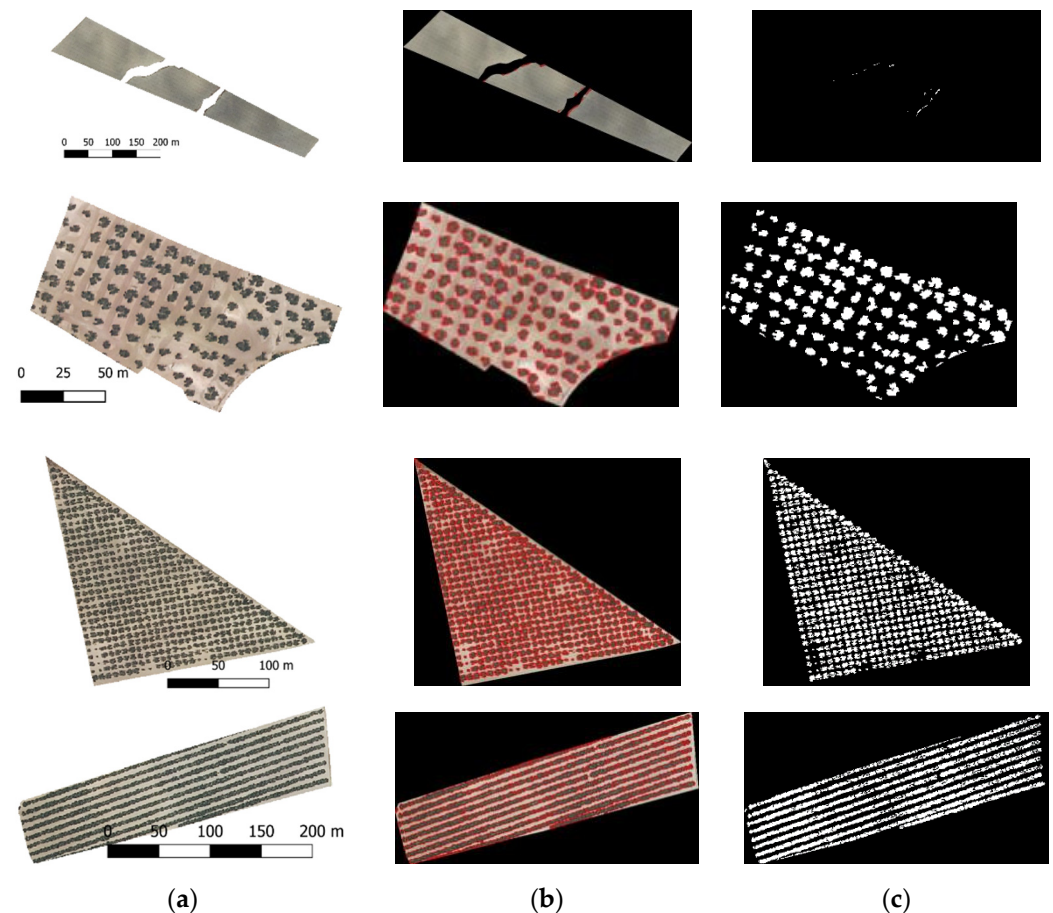
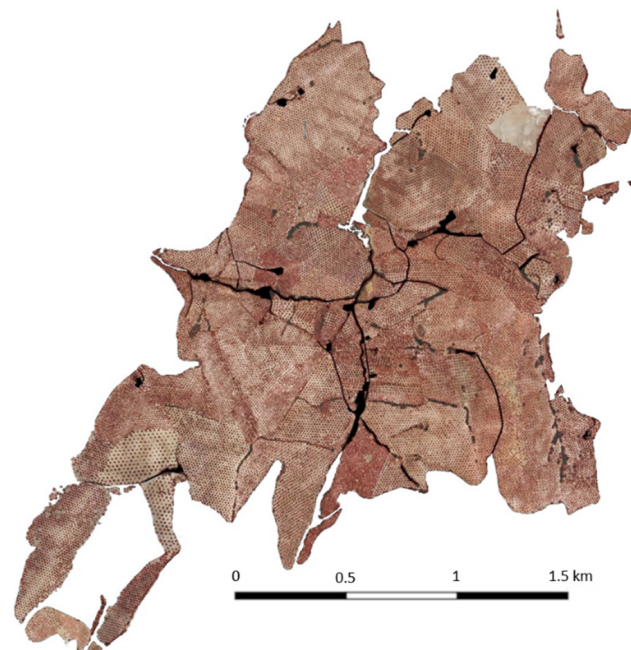


Figure 8. Processing result of 4 plots (14,900,40,60; 23,60,3,88; 14,57,1,58; 14,57,2,49); (a) Input image; (b) Image.tiff at the output; (c) Binary mask with the objects detected.

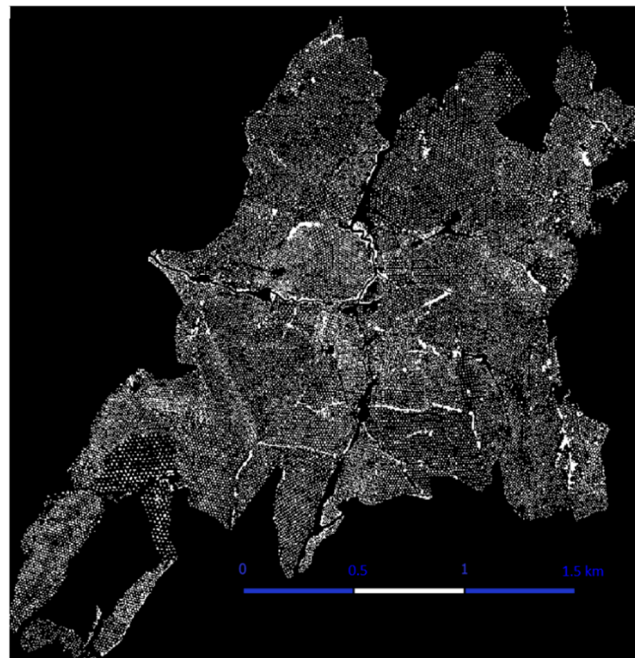
Individualized information was obtained from the units of interest at the polygon and plot level. These processed data form part of the olive grove inventory, which served as support for advanced analytical applications.

Considering the polygon as the study unit allows for a broader view of the olive grove landscape and minimizes edge-processing errors from image analysis, in addition to eliminating double imputation in the tree count of those trees found in the plot edges. Another important aspect is that the analysis at the polygon level allows for a perception of the landscape as a whole, identifying areas with trees and their continuity between plots, as well as other units larger than the plot and of interest for decision-making on a larger scale. From them, the plots can be segregated, to obtain more precise information on the plantation framework and estimation of the crown area. Figure 9 shows an example of a processed polygon, where different plantation frames and treeless areas can be seen.

In the process of integrating and contrasting the information generated by the tool with the different data sources consulted (RAIF; SIGPAC; TRIANA) some non-coherent data were found regarding the cultivated area of olive groves of the RAIF and the SIGPAC. Table 4 shows some records where there is no correspondence between the cultivated area proposed by the RAIF and the cadastral references (SIGPAC). To avoid errors and inconsistency, only the data that were consistent between the two sources were considered from the RAIF. This allowed demonstrating the usefulness of the tool in the analysis processes of different data sources.



(a)



(b)

Figure 9. Example of processing a polygon (14,55,17) belonging to Córdoba: (a) Control image generated by the tool; (b) Binary mask with identified trees.

Table 4. RAIF cultivated area data vs SIGPAC cultivated area.

PROV	MUN	POL	PLOT	Cultivated Area RAIF (ha)	Cultivated Area SIGPAC (ha)
Córdoba	1	7	60	104.56	52.22
Córdoba	25	4	107	146.90	62.47
Córdoba	39	17	9	199.53	8.10
Jaén	2	20	169	52.51	37.63
Jaén	60	1	37	109.10	46.13

After contrasting and integrating the different sources of information, the data included in the olive grove inventory were: (i) crown area, number of trees, FCC, cultivated hectares and tree density from automatic analysis tool; (ii) plantation frame, diameter crown, tree density (no. trees/ha cultivated) of the RAIF; (iii) type of crop, cultivated area, irrigation and geographical limitation of the SIGPAC; (iv) crop type, cultivated area, irrigation, nearest climatic season, planting frame, main variety, planting date, secondary variety and planting date of TRIANA.

The evaluation of 1,519,438 ha of olive groves and the inclusion of metadata from open data sources has allowed for the creation of inventories automatically, which will facilitate evolutionary analyses, and establish the data structure for a more in-depth characterization, identifying peculiarities automatically. In addition, it allows for obtaining general metrics, such as those shown in Figures 10 and 11. Specifically, Figure 10 shows the metrics of the ecological units obtained from the olive grove tool, such as the FCC and the number of trees, and contrasts them with other sources of data consulted, such as the hectares of irrigated land versus those of dry land of the processed area, obtained from the SIGPAC, which allows adding value to the data. Figure 11 shows the estimate of the area by province, with data calculated by the olive grove tool.

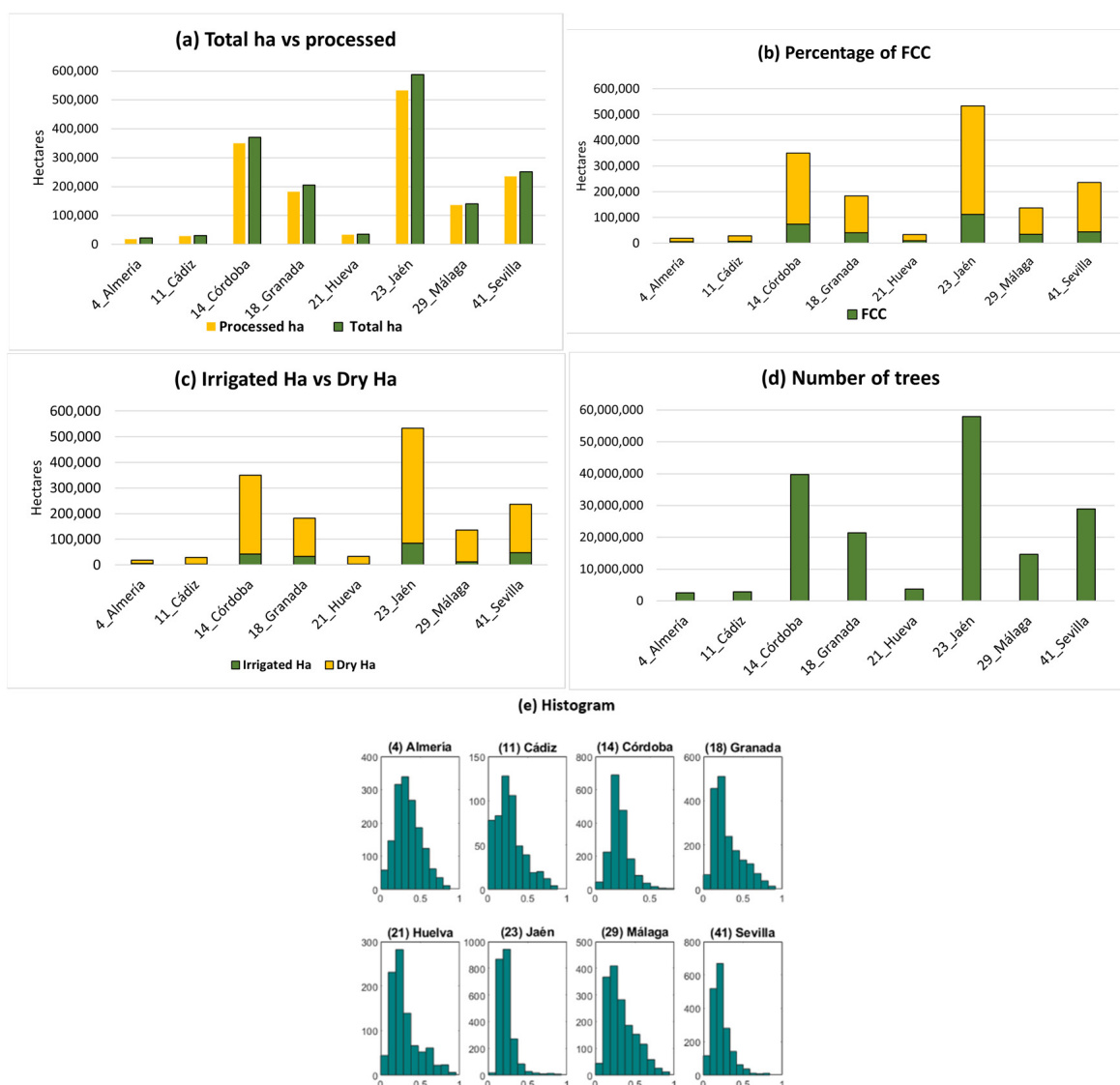


Figure 10. (a) Percentage of ha processed by province; (b) Percentage of FCC obtained by province; (c) Rainfed ha vs. irrigated ha by province; (d) Number of trees per province; (e) Histogram.

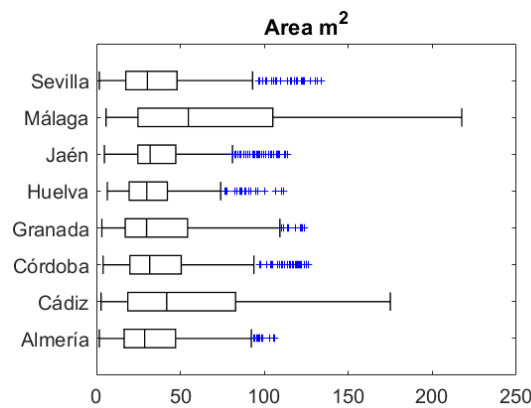


Figure 11. Estimation of the crown area by province.

Additionally, to identify critical points of robustness of the tool, the comparison of calculated tree density and crown diameter was carried out, with one of the most complete sources of the characteristics of olive groves at the plot level (RAIF). To do so, the 200 plots that presented non-null values of these parameters for the year 2019 were selected. Table 5 shows the comparative analysis in a random set of 35 plots of the RAIF of Jaén.

Table 5. Comparative table of the data provided by the RAIF and the estimates made with the developed tool.

ID Prov	ID Parcela			Cultivated Area (ha)	Raif			Cultivated Area (ha)	Calculated		Relative Errors	
	ID Mun	ID Pol	ID Par		Density (Plants/ha)	Canopy Diameter (m)	Density (Plants/ha)		Canopy Diameter (m)	Density	Diameter	
23	1	10	365	4.03	100	7.8	4.1	126.63	6.15	0.27	0.21	
23	1	13	7	0.74	100	5.5	0.75	88.51	5.78	0.11	0.05	
23	2	2	364	2.63	163	4	2.82	177.11	4.69	0.09	0.17	
23	2	4	30	1.97	200	4	2.18	210.31	4.3	0.05	0.07	
23	2	10	245	1.26	170	4	1.25	206.05	4.07	0.21	0.02	
23	2	11	256	1.3	199	4	1.2	221.4	4.03	0.11	0.01	
23	2	17	274	2.39	137	4	2.7	126.27	6.21	0.08	0.55	
23	2	21	236	1.99	157	4	1.36	146.63	5.01	0.07	0.25	
23	2	23	86	2.8	116	4	2.6	131.48	4.72	0.13	0.18	
23	2	29	30	2.31	141	4	2.73	143.05	4.95	0.01	0.24	
23	2	31	202	2.29	188	4	2.3	118.42	4.69	0.37	0.17	
23	2	32	137	2.01	133	4	2	144.8	5.05	0.09	0.26	
23	2	34	67	8.90	168	4	8.93	185.52	4.44	0.1	0.11	
23	2	36	249	1.54	144	4	1.47	135.07	5.67	0.06	0.42	
23	2	55	111	1.24	163	4	1.87	148.28	5.73	0.09	0.43	
23	2	56	29	2.52	148	4	2.62	178.74	5.35	0.21	0.34	
23	2	70	94	9.45	131	4	9.4	132.51	5.92	0.01	0.48	
23	2	71	148	4.64	134	4	5.14	135.38	5.81	0.01	0.45	
23	2	76	68	8.71	129	4	8.77	130.11	5.61	0.01	0.4	
23	2	79	97	2.41	162	4	2.9	169.51	5.53	0.05	0.38	
23	3	6	23	0.91	137	4	0.91	188.12	4.07	0.37	0.02	
23	12	8	189	1.43	100	5.5	1.43	122.41	6.43	0.22	0.17	
23	15	5	880	3.37	140	6.5	3.38	110.29	6.93	0.21	0.07	
23	19	8	338	0.64	115	5	0.64	184.46	5.29	0.60	0.06	
23	19	13	174	0.68	115	5.5	0.69	122.17	6	0.06	0.09	
23	26	15	115	12.67	125	4	12.96	137.11	5.64	0.10	0.41	
23	33	1	180	2.73	152	4	2.8	165.86	4.51	0.09	0.13	
23	33	2	90	1.31	154	4	1.32	161.23	5.44	0.05	0.36	

Table 5. Cont.

ID Prov	ID Parcela			Cultivated Area (ha)	Raif Density (Plants/ha)	Canopy Diameter (m)	Cultivated Area (ha)	Calculated Density (Plants/ha)	Canopy Diameter (m)	Relative Errors	
	ID Mun	ID Pol	ID Par							Density	Diameter
23	33	5	244	0.36	144	4	0.36	145.62	5.11	0.01	0.28
23	33	6	186	0.34	144	4	0.33	163.36	5.08	0.13	0.27
23	33	8	649	0.91	127	4	0.97	165.07	3.95	0.3	0.01
23	53	5	52	3.39	123	6.5	3.39	93.36	6.53	0.24	0
23	53	34	214	1.52	100	8	1.53	122.44	5.38	0.22	0.33
23	63	22	361	3.68	100	5	3.72	105.71	6.96	0.06	0.39
23	63	25	31	5.63	100	4	5.63	100.05	6.43	0.00	0.61

3.3. FCC-NDVI Evaluation

3.3.1. Results Using the Polygon as the Sampling Unit

Table 6 shows the results of the simple linear regression analysis between the NVDI and FCC value data at the cadastral polygon level, aggregated at the province level and for the months of the year with the best results.

Table 6. R-squared, rmse, month, and best-fit simple regression model for each observation area (* p-values: <0.05; Models: S-L: Scikit-Learn; S-M: Stats-Models).

Province	No Polygons	Simple Linear Regression Model					
		β_0	β_1 (NDVI _{mean})	R ²	rmse	Month	Model
4—Almería	1.382	0.0518 *	1.1981 *	0.4302	0.1307	6	S-L
11—Cádiz	399	−0.1650 *	1.6168 *	0.6905	0.0952	8	S-L
14—Córdoba	1.524	−0.0725 *	1.1880 *	0.4883	0.0658	7	S-L
18—Granada	1.650	−0.1542 *	1.6365 *	0.6760	0.0976	6	S-M
21—Huelva	484	−0.1671 *	1.5987 *	0.8150	0.0888	8	S-L
23—Jaén	1.375	−0.1585 *	1.4799 *	0.6156	0.0721	6	S-L
29—Málaga	1.525	−0.1472 *	1.7326 *	0.6777	0.1060	7	S-M
41—Sevilla	1.692	−0.1144 *	1.1885 *	0.5480	0.0759	6	S-M

Figure 12 shows the best R-squared and rmse results and the month for which they were obtained.

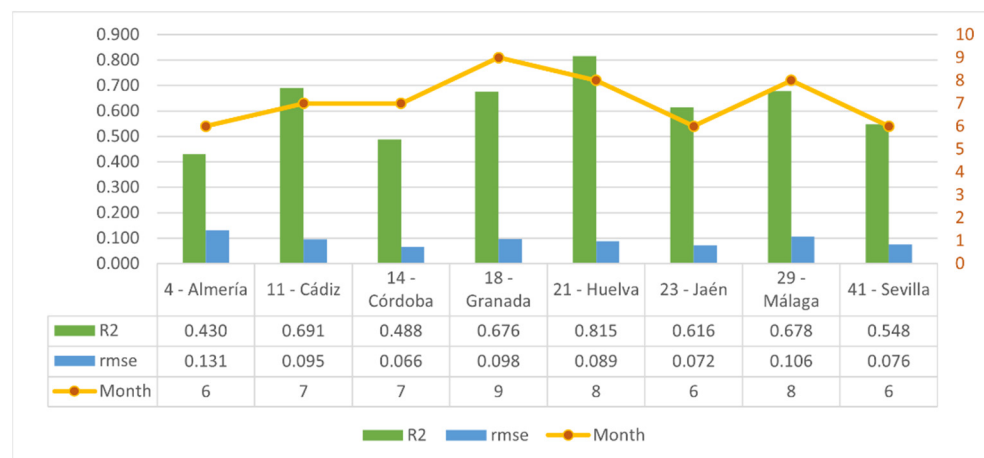


Figure 12. Month in which the best Rsquared and rmse results were obtained for the StatsModel multiple linear regression for each province.

3.3.2. Results Using the Plot as the Sampling Unit

Table 7 shows the results of the simple linear regression analysis of the different models evaluated. The results show that the model that obtained the best approximation was the simple Stats-Models model. In both cases, the p -values and the F-Test were significant.

Table 7. R-squared, rmse, month and best fit model for simple regression (* p -values: <0.05).

Model	β_0	β_1 (NDVI _{mean})	R ²	rmse	Month
Simple S-L	−0.0930 *	1.3436 *	0.7753	0.0538	8
Simple S-M	−0.0931 *	1.3437 *	0.7900	0.0538	8

3.3.3. Results with the Pixel Sampling Unit

Table 8 shows the results of the simple linear regression analysis of the different models evaluated. The results show that the model that obtained the best approximation was the Scikit-Learn model, for the month of August. In both cases the p -values and the F-Test were significant.

Table 8. R-squared, rmse, month and best fit model for simple regression (* p -values: <0.05).

Model	β_0	β_1 (NDVI _{mean})	R ²	rmse	Month
Simple S-L	−0.1677 *	1.3581 *	0.655	0.0729	8
Simple S-M	−0.1678 *	1.3582 *	0.653	0.0729	8

4. Discussion

The objective of this work was to develop a system that allows for creating inventories of olive groves at different scales from the integration of open data sources and calculated automatically through image analysis. As a result, the characterization of 1,519,438 ha of olive groves (92% of the olive grove area of Andalusia) was obtained. This study is in line with [8], where a systematic analysis of the effects on the typology of the olive grove in the countryside of Córdoba and with the strategies of the European Landscape Convention [2] was carried out. In addition, it provides specific information at the polygon and plot level, which serves to be able to evaluate the specific practices at the farm level, a need detected in the studies [7,9].

Our proposal has achieved unified and operational access to the different data sources, allowing their publication and consumption through intuitive interfaces, facing the problem of lack of interoperability indicated in [16,17,22]. To achieve this objective, configurable algorithms have been developed that extract key agronomic information for different attributes, including: (i) crop and phytosanitary information; (ii) access to PNOA high-resolution aerial photogrammetry; (iii) access to images for remote sensing; (iv) time series of the main vegetation indices. All these developments have a great potential to be used for other purposes and crops.

Furthermore, the analysis and integration of the different data sources has allowed their evaluation and comparison. With this, it has been possible to identify some non-coherent data between the different sources studied (see Table 4). Additionally, as can be seen in Table 5, in some cases there are quite a few differences between the data provided by the RAIF and the estimated data, detecting relative errors that reach up to 37%. A detailed analysis of these discrepancies has made it possible to identify that these deviations usually occur in super-intensive olive groves, where the estimation of the area with the methods used loses precision. For this reason, the use of different methodologies for calculating areas based on the plantation framework is proposed for future work. Other discrepancies could be partially explained considering that the data provided by the RAIF could to some extent be the result of rounding, concluding that at least the most important discrepancies with the estimated data would merit a comparison with real data. In the same sense,

the automatic inclusion of this type of measurements would improve the confidence and precision of those collected in the RAIF.

Another point to highlight from the work is the interpretation of data models through image analysis and the use of remote sensing, which is key for the effective and continuous monitoring in large areas [32,33]. The results of our study indicate that the NDVI calculated from the Sentinel-MSI images, particularly in the summer season, has a high relationship with the FCC in all provinces. During this period, the NDVI signal is not influenced by vegetation cover between trees [57,58]. For the same reason, the prediction errors were greater in the remaining seasons (winter, spring and autumn), since they are influenced by the existing vegetation in the streets, which would also allow for characterizing this herbaceous stratum by subtraction.

Our proposal has achieved precise approximations in the different provinces (R-squared between 0.43 and 0.815), similar to those presented in other investigations for other crops [59]. Regarding the results at the plot level, an R-squared of 0.79 was reached. The usefulness of the models at the plot level, in addition to the estimation of the FCC, allows for the identification of the plantation framework, as well as a more precise approximation of the crown area, allowing for the inclusion of more detailed cartographic information in data sources, including existing data, such as RAIF, SIGPAC or TRIANA.

The studies carried out at the pixel level, where R-squared results of 0.655 were achieved, have allowed us to delve into the calculation of spectral mixtures within pixels. Despite the fact that the results were worse than those achieved at the plot level, it is still an attractive line of work to interpret the satellite images at the pixel level and their distribution in the territory.

Regarding the processing of high-resolution image analysis, the tool developed in the study [48] was used, parameterizing it for olive cultivation and the different geographical areas of Andalusia, which has shown the ability to extrapolate this tool to other ecosystems and study areas. In this sense, the shapefiles generated with detailed geographic and agronomic information are a valuable contribution to the inventory of olive groves that allow delving into studies such as sub-pixel classification and the estimation of mixtures, with the aim of classifying and accurately identifying the elements of the olive groves. This raises an interest in multispectral images provided by remote sensing, which is proposed for future studies.

5. Conclusions

The tools and protocols developed make it possible to automate the capture of images of different characteristics and origins, as well as from different open data sources, and integrate them and metadata them so that they can later be used for the development and validation of algorithms that can improve the characterization of the surfaces of olive grove at the plot and cadastral polygon scales.

The proposed system allows for identifying, locating, counting and measuring the fraction of canopy cover (FCC) of olive trees in different locations, plantation frameworks, varieties and tree cultivation techniques. It is robust and useful for carrying out automated inventories of olive groves and incorporating them into decision support strategies.

An inventory of the Andalusian olive grove has been automatically carried out at the level of cadastral polygons and provinces, which has accounted for a total of 1,519,438 hectares and 171,980,593 olive trees, data that have been contrasted with various official statistical sources allowing us to ensure the reliability of this study and even identify some inconsistencies or errors of some sources.

Obtaining singular information at the tree level opens up a great opportunity to systematize the measurement of the impact of various farming practices, the measurement of ecosystem services, the control of compliance with regulations and the granting of public aid.

The ability of Sentinel 2 satellite images to estimate the FCC at the cadastral polygon, plot and 10 × 10 m pixel levels, as well as to perform inventories with temporal resolutions of approximately up to 5 days, has been demonstrated and quantified.

The combination of object-oriented automatic image recognition techniques, with automatic pixel analysis techniques, have allowed us to explore the opportunity of mixture analysis to improve the estimation of olive trees and their characteristics, although it is still necessary to delve further in order to optimize results.

Author Contributions: Conceptualization, C.M.-R., J.E.G.-G. and E.F.-A.; methodology, C.M.-R., J.E.G.-G. and E.F.-A.; software, C.M.-R.; validation, C.M.-R.; formal analysis, C.M.-R.; investigation, C.M.-R., J.E.G.-G. and E.F.-A.; resources, C.M.-R. and J.E.G.-G.; writing—original draft preparation, C.M.-R. and E.F.-A.; writing—review and editing, J.E.G.-G. and E.F.-A.; supervision, J.E.G.-G. and E.F.-A.; funding acquisition, J.E.G.-G. and E.F.-A. All authors have read and agreed to the published version of the manuscript.

Funding: This research received no external funding.

Data Availability Statement: Data are available on request from the first author.

Conflicts of Interest: The authors declare no conflict of interest.

References

- Loumou, A.; Giourga, C. *Olive Groves: “The Life and Identity of the Mediterranean”*; Kluwer Academic Publishers: Alphen aan den Rijn, The Netherlands, 2003; Volume 20.
- Council of Europe Landscape Convention/Official Website. Available online: <https://www.coe.int/en/web/landscape> (accessed on 2 May 2022).
- Guerrero-Casado, J.; Carpio, A.J.; Tortosa, F.S.; Villanueva, A.J. Environmental Challenges of Intensive Woody Crops: The Case of Super High-Density Olive Groves. *Sci. Total Environ.* **2021**, *798*, 149212. [[CrossRef](#)]
- Análisis de La Densidad En Las Plantaciones de Olivar En Andalucía; Servicio de Estudios y Estadísticas; Secretaría General de Agricultura, Ganadería y Alimentación: Spain. 2019. Available online: https://www.juntadeandalucia.es/export/drupaljda/estudios_informes/19/11/An%C3%A1lisis%20densidad%20olivar%20andaluz%20v3.pdf (accessed on 19 July 2022).
- Martínez de Salazar, E.; Fernández, J.A.; Jaramillo, M.A.; Morillo, J.; Rodríguez, M.C. Análisis de Plantaciones Arbóreas Con Programas de Tratamiento de Imagen. Available online: https://intranet.ceautomatica.es/old/actividades/jornadas/XXI/documentos/ja00_052/JA00_052.pdf (accessed on 19 July 2022).
- Mairech, H.; López-Bernal, Á.; Moriondo, M.; Dibari, C.; Regni, L.; Proietti, P.; Villalobos, F.J.; Testi, L. Is New Olive Farming Sustainable? A Spatial Comparison of Productive and Environmental Performances between Traditional and New Olive Orchards with the Model OliveCan. *Agric. Syst.* **2020**, *181*, 102816. [[CrossRef](#)]
- Gómez, J.A.; Montero, A.S.; Guzmán, G.; Soriano, M.A. In-Depth Analysis of Soil Management and Farmers’ Perceptions of Related Risks in Two Olive Grove Areas in Southern Spain. *Int. Soil Water Conserv. Res.* **2021**, *9*, 461–473. [[CrossRef](#)]
- Guzmán, G.; Boumahdi, A.; Gómez, J.A. Expansion of Olive Orchards and Their Impact on the Cultivation and Landscape through a Case Study in the Countryside of Cordoba (Spain). *Land Use Policy* **2022**, *116*, 106065. [[CrossRef](#)]
- Gómez-Limón, J.A.; Picazo-Tadeo, A.J.; Reig-Martínez, E. Eco-Efficiency Assessment of Olive Farms in Andalusia. *Land Use Policy* **2012**, *29*, 395–406. [[CrossRef](#)]
- Durmus, H.; Gunes, E.O. Integration of the Mobile Robot and Internet of Things to Collect Data from the Agricultural Fields. In Proceedings of the 2019 8th International Conference on Agro-Geoinformatics, Agro-Geoinformatics, Istanbul, Turkey, 16–19 July 2019. [[CrossRef](#)]
- Caruso, A.; Chessa, S.; Escolar, S.; Barba, J.; Lopez, J.C. Collection of Data with Drones in Precision Agriculture: Analytical Model and LoRa Case Study. *IEEE Internet Things J.* **2021**, *8*, 16692–16704. [[CrossRef](#)]
- Madhumathi, R.; Arumuganathan, T.; Shruthi, R. A Survey on Wireless Sensor Networks and Instrumentation Techniques for Smart Agriculture. *Lect. Notes Data Eng. Commun. Technol.* **2022**, *68*, 453–467. [[CrossRef](#)]
- Madhumathi, R.; Arumuganathan, T.; Shruthi, R. Internet of Things in Precision Agriculture: A Survey on Sensing Mechanisms, Potential Applications, and Challenges. *Lect. Notes Netw. Syst.* **2022**, *213*, 539–553. [[CrossRef](#)]
- Klaina, H.; Guembe, I.P.; Lopez-Iturri, P.; Campo-Bescós, M.Á.; Azpilicueta, L.; Aghzout, O.; Alejos, A.V.; Falcone, F. Analysis of Low Power Wide Area Network Wireless Technologies in Smart Agriculture for Large-Scale Farm Monitoring and Tractor Communications. *Meas. J. Int. Meas. Confed.* **2022**, *187*, 263–2241. [[CrossRef](#)]
- Joint, R.; Kumar Singh, R.; Hasan Rahmani, M.; Weyn, M.; Berkvens, R. Citation: Communication and Sensing: A Proof of Concept and Datasets for Greenhouse Monitoring Using Article Joint Communication and Sensing: A Proof of Concept and Datasets for Greenhouse Monitoring Using LoRaWAN. *Sensors* **2022**, *22*, 1326. [[CrossRef](#)]
- Gaia-X Domain Agriculture Position Paper Version 1.0. 2021. Available online: https://www.bmwi.de/Redaktion/EN/Publikationen/Digitale-Welt/211116-pp-agriculture.pdf?__blob=publicationFile&v=3 (accessed on 19 July 2022).

17. Roussaki, I.; Doolin, K.; Skarmeta, A.; Routis, G.; Lopez-Morales, J.A.; Claffey, E.; Mora, M.; Martinez, J.A. Building an Interoperable Space for Smart Agriculture. *Digit. Commun. Netw.* **2022**. [CrossRef]
18. Shaping Europe's Digital Future. Available online: <https://op.europa.eu/en/publication-detail/-/publication/33b6e417-53c8-11ea-aece-01aa75ed71a1/language-en> (accessed on 19 July 2022).
19. *A European Strategy for Data*; Brussels, 2020. Available online: <https://eur-lex.europa.eu/legal-content/EN/TXT/?uri=CELEX%3A52020DC0066> (accessed on 19 July 2022).
20. Agricultural Interoperability and Analysis System | ATLAS Project | Fact Sheet | H2020 | CORDIS | European Commission. Available online: <https://cordis.europa.eu/project/id/857125/es> (accessed on 9 April 2022).
21. Building an Interoperable, Data-Driven, Innovative and Sustainable European Agri-Food Sector | DEMETER Project | Fact Sheet | H2020 | CORDIS | European Commission. Available online: <https://cordis.europa.eu/project/id/857202/es> (accessed on 9 April 2022).
22. Objectives-Atlas | Agricultural Interoperability and Analysis System. Available online: <https://www.atlas-h2020.eu/objectives/> (accessed on 9 April 2022).
23. Giray, G.; Catal, C. Design of a Data Management Reference Architecture for Sustainable Agriculture. *Sustainability* **2021**, *13*, 7309. [CrossRef]
24. Murakami, E.; Saraiva, A.M.; Ribeiro, L.C.M.; Cugnasca, C.E.; Hirakawa, A.R.; Correa, P.L.P. An Infrastructure for the Development of Distributed Service-Oriented Information Systems for Precision Agriculture. *Comput. Electron. Agric.* **2007**, *58*, 37–48. [CrossRef]
25. Steinberger, G.; Rothmund, M.; Auernhammer, H. Mobile Farm Equipment as a Data Source in an Agricultural Service Architecture. *Comput. Electron. Agric.* **2009**, *65*, 238–246. [CrossRef]
26. Ouafiq, E.M.; Saadane, R.; Chehri, A.; Jeon, S. AI-Based Modeling and Data-Driven Evaluation for Smart Farming-Oriented Big Data Architecture Using IoT with Energy Harvesting Capabilities. *Sustain. Energy Technol. Assess.* **2022**, *52*, 102093. [CrossRef]
27. Zhaoliang, L.; Huang, W.; Wang, D. Functional Agricultural Monitoring Data Storage Based on Sustainable Block Chain Technology. *J. Clean. Prod.* **2021**, *281*, 124078. [CrossRef]
28. Debauche, O.; Mahmoudi, S.; Manneback, P.; Lebeau, F. Cloud and Distributed Architectures for Data Management in Agriculture 4.0: Review and Future Trends. *J. King Saud Univ.—Comput. Inf. Sci.* **2021**. [CrossRef]
29. Ngo, V.M.; Le-Khac, N.-A.; Kechadi, M.-T. Designing and Implementing Data Warehouse for Agricultural Big Data. In *International Conference on Big Data*; Springer: Berlin/Heidelberg, Germany, 2019.
30. Ouafiq, E.M.; Saadane, R.; Chehri, A. Data Management and Integration of Low Power Consumption Embedded Devices IoT for Transforming Smart Agriculture into Actionable Knowledge. *Agriculture* **2022**, *12*, 329. [CrossRef]
31. Ndao, B.; Leroux, L.; Gaetano, R.; Diouf, A.A.; Soti, V.; Bégué, A.; Mbow, C.; Sambou, B. Landscape Heterogeneity Analysis Using Geospatial Techniques and a Priori Knowledge in Sahelian Agroforestry Systems of Senegal. *Ecol. Indic.* **2021**, *125*, 107481. [CrossRef]
32. Askari, M.S.; McCarthy, T.; Magee, A.; Murphy, D.J. Evaluation of Grass Quality under Different Soil Management Scenarios Using Remote Sensing Techniques. *Remote Sens.* **2019**, *11*, 1835. [CrossRef]
33. Gómez-Giráldez, P.J.; Aguilar, C.; Caño, A.B.; García-Moreno, A.; González-Dugo, M.P. Remote Sensing Estimation of Net Primary Production as Monitoring Indicator of Holm Oak Savanna Management. *Ecol. Indic.* **2019**, *106*, 105526. [CrossRef]
34. Instituto Geográfico Nacional: PNOA (Plan Nacional de Ortografía Aérea). Available online: <http://www.ign.es/wms-inspire/pnoa-ma> (accessed on 19 July 2022).
35. Gorelick, N.; Hancher, M.; Dixon, M.; Ilyushchenko, S.; Thau, D.; Moore, R. Google Earth Engine: Planetary-Scale Geospatial Analysis for Everyone. *Remote Sens. Environ.* **2017**, *202*, 18–27. [CrossRef]
36. González-Dugo, M.P.; Escuin, S.; Cano, F.; Cifuentes, V.; Padilla, F.L.M.; Tirado, J.L.; Oyonarte, N.; Fernández, P.; Mateos, L. Monitoring Evapotranspiration of Irrigated Crops Using Crop Coefficients Derived from Time Series of Satellite Images. II. Application on Basin Scale. *Agric. Water Manag.* **2013**, *125*, 92–104. [CrossRef]
37. Jiang, Z.; Huete, A.R.; Didan, K.; Miura, T. Development of a Two-Band Enhanced Vegetation Index without a Blue Band. *Remote Sens. Environ.* **2008**, *112*, 3833–3845. [CrossRef]
38. Plant, R.E. Site-Specific Management: The Application of Information Technology to Crop Production. *Comput. Electron. Agric.* **2001**, *30*, 9–29. [CrossRef]
39. Chandra, P. Performance Evaluation of Vegetation Indices Using Remotely Sensed Data. *Int. J. Geomat. Geosci.* **2011**, *2*, 231–240.
40. Scheftic, W.; Zeng, X.; Broxton, P.; Brunke, M. Remote Sensing Intercomparison of Seven NDVI Products over the United States and Mexico. *Remote Sens.* **2014**, *6*, 1057–1084. [CrossRef]
41. Gopperundevi, M.; Udhayakumar, C.S.; Menaka, C.; Ravindran, A.; Kannan, V. Inventory of Sathanur Command Area for Management of Irrigation System Using Remote Sensing and Geographical Information System. *J. Mod. Biotechnol.* **2012**, *1*, 31–36.
42. Junta de Andalucía: Consejería de Agricultura, G.P. y D.Sostenible. Descarga de Información Geográfica SIGPAC. Available online: <https://www.juntadeandalucia.es/organismos/agriculturaganaderiapescaydesarrollosostenible/servicios/sigpac/visor/paginas/sigpac-descarga-informacion-geografica-shapes-provincias.html> (accessed on 5 March 2022).
43. Junta de Andalucía: Consejería de Agricultura, G.P. y D.Sostenible. Datos Obtenidos Del Seguimiento de Plagas y Enfermedades En Las Estaciones de Control Biológico [2006–2021] Red de Alerta e Información Fitosanitaria (RAIF). Available online: <https://www.juntadeandalucia.es/datosabiertos/portal/dataset/raif> (accessed on 5 March 2022).

44. Junta de Andalucía: Consejería de Agricultura, G.P. y desarrollo S. Programa TRIANA: Tratamientos Integrados En Andalucía En Agricultura. Available online: <https://www.juntadeandalucia.es/organismos/agriculturaganaderiapescaydesarrollosostenible/areas/agricultura/sanidad-vegetal/paginas/produccion-integrada-atrias-programas-triana.html> (accessed on 5 March 2022).
45. Sentinel Application Platform (SNAP). Available online: <http://step.esa.int/main/toolboxes/snap/> (accessed on 19 July 2022).
46. Image Processing Toolbox—MATLAB. Available online: <https://www.mathworks.com/products/image.html> (accessed on 25 March 2022).
47. OpenEarth: Openearthtools. Available online: <https://svn.oss.deltares.nl/repos/openearthtools/trunk/matlab/applications/> (accessed on 19 July 2021).
48. Martínez-Ruedas, C.; Guerrero-Ginel, J.E.; Fernández-Ahumada, E. A Methodology for Automatic Identification of Units with Ecological Significance in Dehesa Ecosystems. *Forests* **2022**, *13*, 581. [[CrossRef](#)]
49. Ministerio de Agricultura, Pesca y Alimentación (MAPA). Catálogo de Servicios de Visualización Inspire Del SIGPAC: Servicios WMS. Available online: https://www.mapa.gob.es/es/cartografia-y-sig/ide/directorio_datos_servicios/agricultura/servicios-wms-sigpac/wms_sigpac.aspx (accessed on 5 March 2022).
50. Gougeon, F.A.; Leckie, D.G. *Forest Information Extraction from High Spatial Resolution Images Using an Individual Tree Crown Approach*; Pacific Forestry Centre: Victoria, BC, Canada, 2003; ISBN 0662332725.
51. Moritz, S.; Bartz-Beielstein, T. ImputeTS: Time Series Missing Value Imputation in R. *R J.* **2017**, *9*, 207–218. [[CrossRef](#)]
52. Naveen, S.; Aiswarya, V.A. Image Denoising by Fourier Block Processing and Wiener Filtering. *Procedia Comput. Sci.* **2015**, *58*, 683–690. [[CrossRef](#)]
53. Motwani, M.C.; Gadiya, M.C.; Motwani, R.C.; Harris, F.C. Survey of Image Denoising Techniques. *Proc. GSPX* **2004**, *27*, 27–30. [[CrossRef](#)]
54. Haralick, R.M.; Shapiro, L.G. Image Segmentation Techniques. *Comput. Vis. Graph. Image Processing* **1985**, *29*, 100–132. [[CrossRef](#)]
55. Pal, N.R.; Pal, S.K. A Review on Image Segmentation Techniques. *Pattern Recognit.* **1993**, *26*, 1277–1294. [[CrossRef](#)]
56. Lu, D.; Weng, Q. A Survey of Image Classification Methods and Techniques for Improving Classification Performance. *Int. J. Remote Sens.* **2007**, *28*, 823–870. [[CrossRef](#)]
57. Gallardo, A. Effect of Tree Canopy on the Spatial Distribution of Soil Nutrients in a Mediterranean Dehesa. *Pedobiologia* **2003**, *47*, 117–125. [[CrossRef](#)]
58. Grant, C.C.; Scholes, M.C. The Importance of Nutrient Hot-Spots in the Conservation and Management of Large Wild Mammalian Herbivores in Semi-Arid Savannas. *Biol. Conserv.* **2006**, *130*, 426–437. [[CrossRef](#)]
59. Tenreiro, T.R.; García-Vila, M.; Gómez, J.A.; Jiménez-Berni, J.A.; Fereres, E. Using NDVI for the Assessment of Canopy Cover in Agricultural Crops within Modelling Research. *Comput. Electron. Agric.* **2021**, *182*, 106038. [[CrossRef](#)]